Drought impacts on photosynthesis, isoprene emission and atmospheric formaldehyde in a mid-latitude forest

Yiqi Zheng[1], Nadine Unger[2], Jovan M. Tadić[3,*], Roger Seco[4], Alex B. Guenther[4], Michael P. Barkley[5], Mark J. Potosnak[6], Lee Murray[7], Anna M. Michalak[3], Xuemei Qiu[3], Saewung Kim[4], Thomas Karl[8], Lianhong Gu[9], Stephen G. Pallardy[10]

[1] Department of Geology and Geophysics, Yale University, New Haven, CT 06511, USA
[2] College of Engineering, Mathematics and Physical Sciences, University of Exeter, Exeter, UK
[3] Department of Global Ecology, Carnegie Institution for Science, Stanford, CA 94305, USA
[4] Department of Earth System Science, University of California, Irvine, CA 92697, USA
[5] EOS group, Department of Physics and Astronomy, University of Leicester, Leicester, UK
[6] Environmental Science and Studies, DePaul University, Chicago, IL 60614, USA
[7] Department of Earth and Environmental Sciences, University of Rochester, NY 14627, USA
[8] Institute of Meteorology and Geophysics, University of Innsbruck, Innsbruck, Austria
[9] Environmental Sciences Division, Oak Ridge National Laboratory, Oak Ridge, TN 37831, USA
[10] Department of Forestry, University of Missouri, Columbia, MO 65211, USA
[*] Now at Earth and Environmental Sciences Area, Lawrence Berkeley National Lab, Berkeley, CA 94720, USA
Correspondence to: Y. Zheng (yiqi.zheng@yale.edu)

Abstract

Isoprene plays a critical role in air quality and climate. Photosynthesis (gross primary productivity, GPP) and formaldehyde (HCHO) are both related to isoprene emission at large spatiotemporal scales, but neither is a perfect proxy. We apply multiple satellite products and site-level measurements to examine the impact of water deficit on the three interlinked variables at the Missouri Ozarks site during a 20-day mild dryness stress in summer 2011 and a 3-month severe drought in summer 2012. Isoprene emission shows opposite responses to the short- and long-term droughts, while GPP was substantially reduced in both cases. In 2012, both remote-sensed solar-induced fluorescence (SIF) and satellite HCHO column qualitatively capture reductions in flux-derived GPP and isoprene emission, respectively, on weekly to monthly time scales, but with muted responses. For instance, as flux-derived GPP approaches zero in late summer 2012, SIF drops by 29~33% (July) and 19~27% (August) relative to year 2011. A possible explanation is that electron transport and photosystem activity are maintained to a certain extent under the drought stress. Similarly, flux tower isoprene emissions in July 2012 are 54% lower than July 2011, while the relative reductions in July for 3 independent satellite-derived HCHO data products are 27%, 12% and 6%, respectively. We attribute the muted HCHO response to a photochemical feedback whereby reduced isoprene emission increases the oxidation capacity available to generate HCHO from other volatile organic compound sources. Satellite SIF offers a potential alternative indirect method to monitor isoprene variability at large spatiotemporal scales from space, although further research is needed under different environmental conditions and regions. Our analysis indicates that fairly moderate reductions in satellite SIF and HCHO column may imply severe drought conditions at the surface.

Keywords

The Missouri Ozarks; satellite; formaldehyde; gross primary productivity; solar-induced fluorescence; water stress.

Highlights

1. Satellite SIF response to severe 2012 drought muted relative to flux tower GPP
2. Satellite HCHO column response to 2012 drought muted relative to isoprene emission
3. Satellite SIF and surface isoprene emission show strong correlation on monthly scales

1. Introduction

Terrestrial vegetation emits over 500 Tg per year of isoprene [*Guenther et al.*, 2006]. The rapid photo-oxidation of isoprene alters the concentration and variability of methane, tropospheric ozone and secondary organic aerosol, thus playing a critical role in both air quality and climate [*Carslaw et al.*, 2010; *Unger*, 2014b]. Spatiotemporal variability in isoprene emission rate depends upon vegetation type, physiological status, leaf age and meteorological conditions, including temperature and soil moisture, and is therefore sensitive to climate change and land cover change [*Unger*, 2014a; *Heald and Spracklen*, 2015]. The frequency and intensity of drought is projected to increase in the coming century under future climate change [*Cook et al.*, 2014]. Accurate simulation of future air quality and climate requires improving the understanding of isoprene emission response to drought conditions [*Monson et al.*, 2007].

Two processes are related to isoprene emission at large spatiotemporal scales: photosynthesis and atmospheric formaldehyde (HCHO) formation. Isotopic labeling studies have shown that 70-90% of isoprene production is directly linked to photosynthesis (gross primary productivity, GPP) that provides the supply of energy and precursors for biosynthesis in the chloroplast [*Delwiche and Sharkey*, 1993; *Karl et al.*, 2002; *Affek and Yakir*, 2003]. Yet, the situation is complex because isoprene emission may be decoupled from the photosynthetic flow under specific conditions, including water stress [*Pegoraro et al.*, 2005]. Under short-term and mild droughts, photosynthetic rate instantaneously decreases due to limited stomatal conductance; while isoprene emission is not necessarily impacted because photosynthetic electron transport is not inhibited [*Fall and Monson*, 1992; *Niinemets*, 2010], and can even increase due to warm leaf temperatures [e.g. *Pegoraro et al.*, 2005]. Under prolonged or severe drought stress, after a lag relative to the photosynthesis reduction, isoprene emission declines because of inadequate carbon availability [*Sharkey and Loreto*, 1993; *Brüggemann and Schnitzler*, 2002; *Funk et al.*, 2005]. *Ryan et al.* [2014] suggested that isoprene emission protected photosynthesis but further reduced productivity. Recent advances in remote sensing of solar-induced fluorescence (SIF) open up the possibility for direct global observational constraints on photosynthesis [e.g. *Meroni et al.*, 2009; *Frankenberg et al.*, 2011; *Joiner et al.*, 2013; *Garbulsky et al.*, 2014; *Guanter et al.*, 2014; *Parazoo et al.*, 2014]. Some studies have suggested that SIF offers a better indicator of plant productivity than other satellite-based vegetation indices such as the Enhanced Vegetation Index (EVI) and Normalized Difference Vegetation Index (NDVI), because it is more closely related to physiology and function than plant structure as in the case of EVI and NDVI [*Yoshida et al.*, 2015; *Walther et al.*, 2016]. Therefore, SIF is expected to provide more reliable information under plant stress conditions including drought. The reliability of SIF in representing GPP under water stress and the novel potential for SIF to evaluate isoprene emission responses warrants further investigation.

Many studies have pioneered the use of remotely-sensed tropospheric HCHO columns as a proxy for surface isoprene emission [*e.g. Barkley et al.*, 2008*; Fu et al.*, 2007*; Marais et al.*, 2012; *Palmer et al.*, 2006], as HCHO is a high-yield product of isoprene oxidation and has a short lifetime of a few hours against photolysis and oxidation by hydroxyl radical (OH). The validation is, however, challenging because of the large uncertainties associated with the HCHO retrieval and the limited availability of ground measurements [*Zhu et al.*, 2016]. Water availability has contrasting impacts on atmospheric HCHO concentration versus biogenic

emissions of isoprene. For example, precipitation may wash out oxidants, reactive carbon and nitrogen oxide compounds, thus diminishing HCHO formation from isoprene oxidation. HCHO itself may undergo wet deposition [*Báez et al.*, 1993]. *Duncan et al.* [2009] found an anti-correlation between monthly HCHO columns and topsoil moisture in the central and eastern US. *Zheng et al.* [2015b] using isoprene emission models that account for soil moisture dependence showed that the growing season interannual variability of isoprene emission is coupled with photosynthesis and not HCHO column. Direct observational evidence of the impact of water availability on photosynthesis, isoprene and HCHO is needed to better understand the coupled vegetation-chemistry-climate system.

Two recent isoprene measurement campaigns were conducted in the Missouri Ozarks [*Potosnak et al.*, 2014; *Seco et al.*, 2015], a mid-latitude oak-dominated forest in central US, which is known as the "isoprene volcano" [*Wiedinmyer et al.*, 2005; *Carlton and Baker*, 2011]. *Potosnak et al.* [2014] reported the highest ecosystem isoprene emission in Ozarks in summer 2011 compared to all other canopy-scale reports, which was attributed to the previous days' temperature and light regimes as well as short-term drought stress. In contrast, *Seco et al.* [2015] found strongly suppressed photosynthesis and isoprene emission in the 2012 summer, which suffered progressing drought conditions. In this study, we re-examine the impacts of the 2011 and 2012 drought episodes with a new focus on the responses of the satellite-based indicators: SIF and HCHO columns.

2. Method

2.1 Observational data sets

2.1.1 Site description and meteorological data

The Missouri Ozarks flux (MOFLUX) site, part of the AmeriFlux network [*Baldocchi et al.*, 2001], is located in the University of Missouri Baskett Wildlife Research and Education area in central Missouri (latitude 38.74°N, longitude 92.20°W, elevation 219 m). The site is dominated by deciduous broadleaf tree species especially oak (more than 60%). The climate in this area is warm, humid and continental. Moderate to severe droughts commonly occur in summer [*Gu et al.*, 2006, 2015, 2016].

In this study, all site-level meteorological data (2007-2013) at the MOFLUX site are from the AmeriFlux website (http://ameriflux.ornl.gov/fullsiteinfo.php?sid=64, retrieved on August 6, 2015). We average all these 1-hour datasets from 10:00 to 16:00 local time for each day to calculate the corresponding midday average values, except that for precipitation the whole 24-hour period of each day was summed.

We use the gridded monthly precipitation product from the NASA Modern Era Retrospective Analysis for Research and Applications (MERRA) [*Rienecker et al.*, 2011] to calculate the 3-month Standardized Precipitation Index (SPI). The SPI is an index to evaluate drought severity [*Guttman*, 1999], calculated based on seasonal precipitation anomalies (3 months preceding the target month) and standardized by long-term (1979-2013) precipitation variations (https://www.ncl.ucar.edu/Applications/spi.shtml).

2.1.2 Isoprene measurements

We use isoprene emission datasets from two recent campaigns at the MOFLUX site in 2011 [*Potosnak et al.*, 2014] and 2012 summers [*Seco et al.*, 2015]. The missing data from day 222 to 229 (August 10-17) in 2011 is due to equipment failure related to the ozone generator [*Potosnak et al.*, 2014]. We use the local time 10:00-16:00 average for each day as the representative midday average values in our analysis.

2.1.3 Site-level GPP

Gross primary productivity (GPP) is the total amount of carbon assimilated by the photosynthetic machinery without taking into account non-photo respiratory fluxes from the ecosystem. We apply the New REddyProcWeb online tool (http://www.bgc-jena.mpg.de/bgi/index.php/Services/REddyProcWeb, accessed on May 20, 2016) to derive site-level GPP from AmeriFlux measurement of net ecosystem exchange (NEE) and other meteorological conditions, in which the algorithm is based on *Reichstein et al.*, [2005].

2.1.4 Satellite-based SIF

Absorbed photosynthetically active radiation (APAR, 400-700 nm) drives photosynthesis, and at the same time can be dissipated into heat and re-radiated at longer wavelengths (660-800 nm). Such solar-induced fluorescence (SIF) can be measured from space and exhibits a strong linear correlation with GPP [e.g. *Frankenberg et al.*, 2011]. We use two regional gridded SIF data sets in 2007-2013 that are retrieved from the Global Ozone Monitoring Experiment-2 (GOME-2) instrument on board Meteorological Operational Satellite-A (MetOp-A) [e.g. *Joiner et al.*, 2013]. One dataset applies a spatial moving window block kriging method (SIF_sp) [*Tadić et al.*, 2015], and the other applies a spatio-temporal kriging method (SIF_st) [*Tadić et al.*, 2017], both with a spatial resolution of 1°×1°.

Product	Instrument (Satellite)	Post-processing model	Model type	Year-specific AMFs?	Available period
OMI-std [*González Abad et al.*, 2015]	OMI (Aura)	GEOS-Chem [*Bey et al.*, 2001]	Chemical-transport	No (fixed at 2007)	2007-2013
OMI-GC (in courtesy of L. Murray)	OMI (Aura)	GEOS-Chem	Chemical-transport	Yes	2007-2012
OMI-IM [*De Smedt et al.*, 2015]	OMI (Aura)	IMAGES [*Muller and Stavrakou*, 2005]	Chemical-transport	Yes	2007-2013
GOME2-IM [*De Smedt et al.*, 2012]	GOME2 (MetOp-A)	IMAGES	Chemical-transport	Yes	2007-2013

Table 1. Products of satellite-based tropospheric HCHO vertical columns. Abbreviations are listed below. OMI: the Ozone Monitoring Instrument. GOME2: the Global Ozone Monitoring Experiment-2. MetOp-A: the Meteorological Operational satellite-A programme.

2.1.5 Satellite-based tropospheric HCHO vertical columns

Satellite-based tropospheric HCHO vertical columns have been used to estimate surface isoprene emission variations. Converting vertical HCHO columns from retrieved slant columns requires a priori modeled air mass factors (AMFs). In this study, we examine four products of daily HCHO columns that are retrieved from two satellite instruments: OMI (Ozone Monitoring Instrument) on board NASA Aura (equatorial crossing time 1:30 pm) and GOME-2 on board MetOp-A (equatorial crossing time 9:30 am). Details are summarized in Table 1. We regrid all datasets to 1° × 1° and use the grid point above the MOFLUX site in 2007-2013 summers.

2.2 Photochemical box model simulations

We apply a 0-D chemical box model BOXMOX [*Knote et al.*, 2014] version 1.0 to examine the HCHO concentration responses to changes in isoprene emission, air temperature and water vapor concentration. BOXMOX is an extension to the Kinetic PreProcessor (KPP, http://people.cs.vt.edu/~asandu/Software/Kpp/) that allows simulations of species concentrations within boundary layer. In BOXMOX, we use the same O_3-NO_x-CO-VOC gas-phase chemistry mechanism as in the Community Atmosphere Model with Chemistry (CAM5-chem, [*Lamarque et al.*, 2012; *Tilmes et al.*, 2015]), which borrows heavily from MOZART-4 [*Emmons et al.*, 2010] and contains an explicit description of radical cycling (especially OH and HO_2), NO_x chemistry and a representation of the main VOC species. Halogen chemistry and heterogeneous reactions (e.g. on aerosol surfaces) are switched off in this study. Hourly photolysis rates are fixed to WRF-chem 3.5.1 values and do not respond to local measured meteorology at the MOFLUX site. We use the same emission inventory as described in *Zheng et al.* [2015a] and *Lamarque et al.* [2012]. For CO and the short-lived species SO_2, NH_3 and 14 anthropogenic volatile organic compounds (VOCs), their hourly surface emissions are set to a single value without diurnal variations, which is the value of the grid box over the MOFLUX site and is averaged from 2000 to 2010. The monoterpene emission is replaced with the observed hourly emission from the 2012 campaign at the MOFLUX site [*Seco et al.*, 2015], averaged over the whole summer (June-July-August, JJA). The nitrogen oxides (NO_x) emission is replaced with the hourly emission from 2005 U.S. National Emission Inventory (NEI2005, available online ftp://aftp.fsl.noaa.gov/divisions/taq/emissions_data_2005/). We conduct additional sensitivity experiments in which the NEI2005 NO_x emission is multiplied by a factor of 0.2, 0.5 or 2. We assume a typical diurnal pattern for boundary layer height. The longer-lived species CH_4 and CO are assigned to 1800 ppbv and 120 ppbv as initial values and are allowed to change over time, though the changes would be small within the simulation time (48 hours). The above emissions, initial concentrations and environmental variables are identical for all case simulations in this study.

We performed 6 groups of simulations, each representing a month in summer 2011 or 2012. We use observed hourly air temperature (T_a, Section 2.1.1) and isoprene emission (Iemis, Section 2.1.2), averaged for the corresponding month. The water vapor concentration (H_2O), held constant in each simulation, is also calculated as the observed monthly mean value in corresponding month. Each group has 4 simulations:

Case 1: T_a, H_2O and Iemis are all set to their 2011 levels in corresponding month.

Case 2: T_a is set to it value in 2012; H_2O and Iemis remain at their 2011 levels.

Case 3: T_a and H_2O are set to 2012 levels; Iemis remains at its 2011 level.

Case 4: T_a, H_2O and Iemis are all set to their 2012 values in corresponding month.

Each simulation has been run for 48 hours. We use the last 24 hours for analysis.

3. Results

3.1 Responses of site-level photosynthesis and isoprene emission to drought

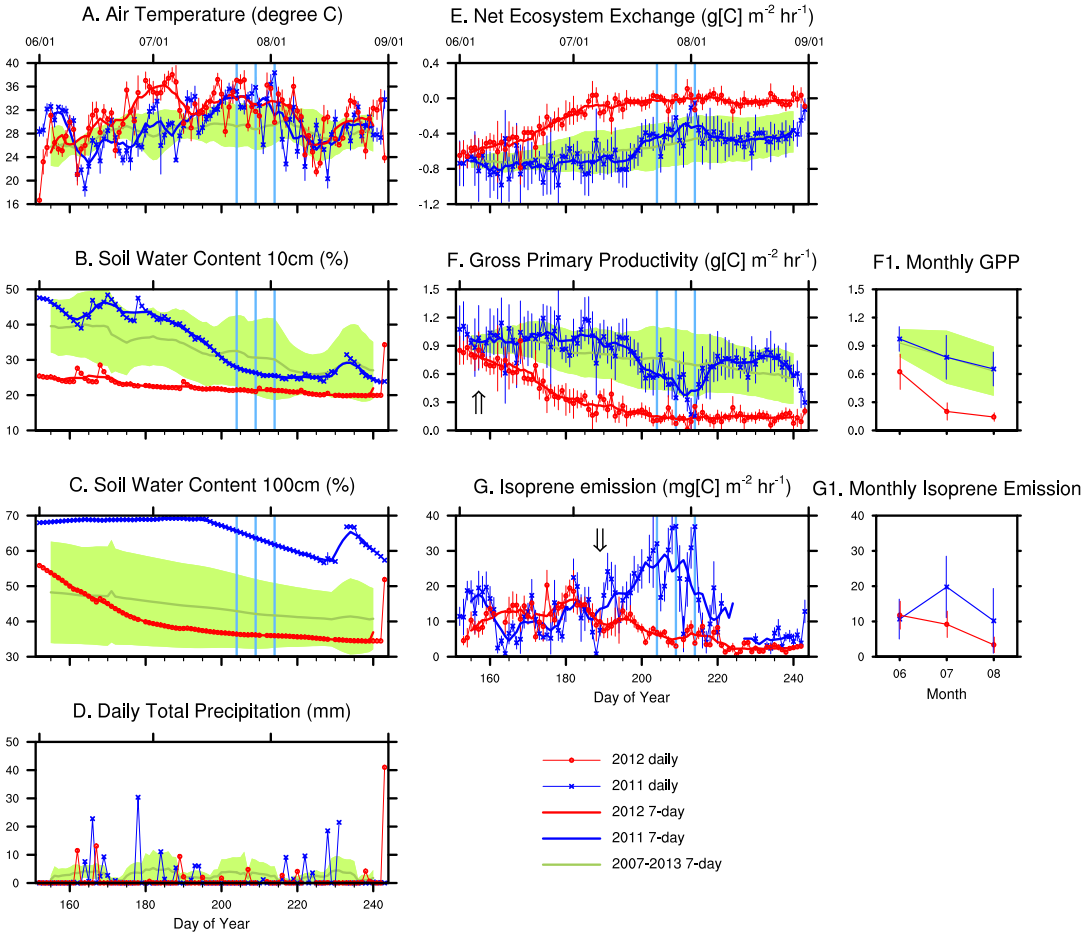

Figure 1. Time-series of midday meteorological variables, net ecosystem exchange (NEE), gross primary productivity (GPP) and isoprene emission at the MOFLUX site in June-July-August. The midday values are calculated as the 10:00-16:00 local time averages, except for precipitation the whole 24 hour period of each day is summed. Green shading represents the multi-year variation of the 7-day running mean values. Error bars in the daily time-series plots represent the variation within 10:00-16:00 each day. Error bars in the monthly plots represent the 1 standard deviation of day-to-day variation within each month. The vertical light blue lines indicate three hot events in 2011. The black arrows show the time from which the 2012 values start to deviate from the corresponding 2011 values.

The MOFLUX site has experienced distinct water conditions in 2011 and 2012 summers. The site-level midday air temperature, soil water content measured at two soil depths 10cm and 100cm (SWC1 and SWC2) and daily total precipitation are shown in Fig. 1. The 2011 summer is

overall wet, except for a 3-week dry and hot period in late July (day 195~215). No precipitation in this period results in the slightly below-normal topsoil moisture, suggesting a short-term mild heat and dryness stress. The deep soil moisture is consistently ~1.5 times larger than the multi-year average. The Ozarks suffered severe drought conditions in summer 2012, which is part of a historical drought in the central US since record keeping began in 1895 [*Rippey*, 2015]. The 2012 summer is warmer than usual with a mean June-July-August (JJA) air temperature of 30.8°C, 2.6°C higher than the 2007-2013 average. The topsoil moisture deficit is largest in June 2012 and consistently equals or exceeds the one standard deviation of multi-year variation. The deep layer soil is wetter than its climatology before June, but decreases quickly in early June and stays below normal values for the rest of the summer. This 3-month long, severe drought condition is partly relieved by a large rain event that occurred in the last day of August (Fig. 1D). The impacts of the slight intra-seasonal drying trend from June to August are not analyzed in the present study.

The site-level measured photosynthesis and isoprene emission show opposite responses to the 3-week hot and dry period in late July, 2011. GPP falls below normal, and reaches minima during the three hottest days (day 204, 209, 214, vertical blue lines in Fig. 1). This phenomenon could be attributed to the temperatures that are higher than the GPP thermal optima (usually 25-30°C, e.g. [*Sharkey and Loreto*, 1993]) and the below-normal topsoil moistures. Isoprene emissions instead show a burst induced by high leaf temperatures. During these short-time (daily) events, GPP and isoprene emissions are anti-correlated because they differ in thermal optima and respond differently to short-term water deficit.

In the severe drought conditions of 2012, both photosynthesis and isoprene emissions decrease considerably (Fig. 1E and 1F). NEE and GPP are close to 0 in the middle to late summer. The 2012 GPP is consistently lower than the 2011 GPP since mid-June, with a relative difference of -20%, -97% and -38% in June, July and August, respectively. Isoprene fluxes in July and August 2012, despite the high temperatures, are dramatically lower than in 2011 by a factor of 2 to 3 (Fig. 1G) and also lower than the June values of the same year. The isoprene emissions are 10 and 3.5 mg[C] m^{-2} hr^{-1} in 2012 July and August, as compared to 20 and 11 mg[C] m^{-2} hr^{-1} in 2011, respectively. The 2012 and 2011 isoprene emissions do not show significant differences until the second week of July. This pattern indicates that the starting time of isoprene reduction is delayed by a few weeks compared to GPP, whose 2012 values deviate from the 2011 values since the second week of June (Fig. 1F and 1G, black arrows). This observation is consistent with findings from previous studies [*Fall and Monson*, 1992; *Niinemets*, 2010, *Seco et al.*, 2015]. At such longer (monthly) time scales, GPP and isoprene emission respond in the same direction.

3.2 Response of satellite SIF

SIF, as an alternative proxy for GPP from space, successfully capture the GPP reductions under water stress (Fig. 2), which is consistent with a previous study [*Sun et al.*, 2015]. The SIF (especially SIF_st, processed using spatiotemporal kriging method) reductions in summer 2012 compared to 2011 are mostly statistically significant with respect to day-to-day variations, i.e. p-values for student's t-test are smaller than 0.05 (Table 2). SIF_st performs better at reproducing the variability in the site-level flux tower GPP than SIF_sp (processed using spatial kriging method). At monthly scale, SIF_sp and SIF_st show significant correlations with in-situ GPP

with r^2 of 0.38 and 0.76, respectively. At weekly scales, Both datasets reproduce the lower in-situ GPP values in late July 2011 compared to early July. At daily time scales, only SIF_st captures the day-to-day GPP variations (r^2=0.52).

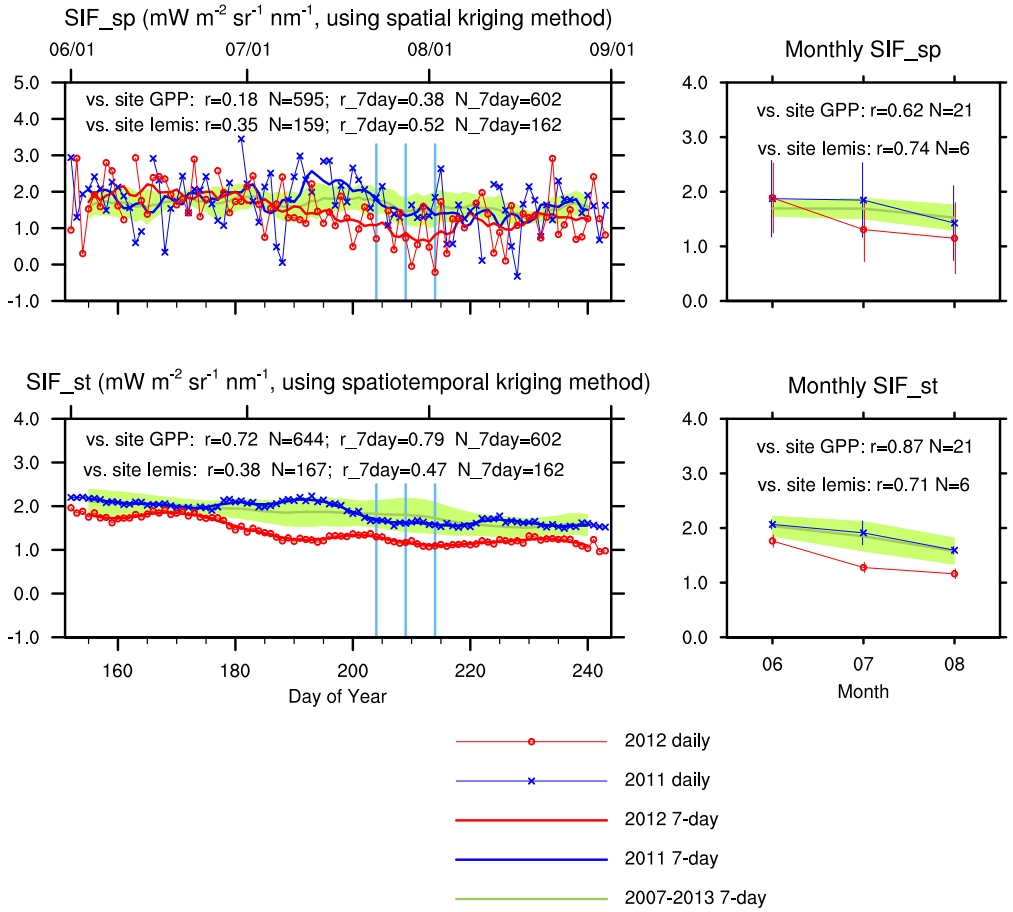

Figure 2. Time-series of GOME-2 solar-induced fluorescence (SIF) over the MOFLUX site. Green shading represents the multi-year variation. The vertical light blue lines indicate three hot events in 2011. The correlation coefficients r against site-level GPP and isoprene emission (Iemis) are calculated using daily, 7-day running mean and monthly mean for SIF_sp and SIF_st. The error bars in the monthly plots represent the 1 standard deviation of day-to-day variations within each month.

The SIF and GPP responses are in the same direction but to a varying degree. The 2012-2011 differences for SIF_sp and SIF_st in July are -29% and -33% (Table 2), much smaller than that of GPP (-97%). The monthly SIF-to-GPP regression lines are: SIF_sp=0.49*GPP+1.26 and SIF_st=1.00*GPP+1.04, respectively. The non-zero SIF-to-GPP intercept indicates a minimum SIF value even when GPP gets close to zero under stressed circumstances. This phenomenon is not explicitly emphasized by previous studies comparing satellite SIF with gridded or site-level GPP [e.g. *Voigt et al.*, 2009; *Frankenberg et al.*, 2011; *Xu et al.*, 2015; *Yang et al.*, 2015], but is consistent with *Lee et al.* [2015]. The muted SIF response may be because electron transport and photosystem activity are maintained even though plant metabolic pathways have shut down [*Lawlor and Tezara*, 2009]. Other possible reasons include the different spatial scales of the data products (~1km for GPP and ~100km for SIF products) and the uncertainties associated with the

GPP derivation and SIF retrieval. Though to different extents, site-level GPP and SIF products indicate a strong reduction in photosynthesis, which is a result of substantial soil water deficit conditions associated with high temperatures and lack of precipitation.

The reductions in both GPP and isoprene emission under long-term stress indicates a positive coupling of the two quantities at long temporal scales. To explore the potential use of satellite photosynthesis datasets as a proxy for surface isoprene emission, we calculate the correlation between isoprene emissions and the two SIF products (Fig. 2). Neither of the SIF products reproduce the short-term (daily to weekly) variations of isoprene emissions, because photosynthesis and isoprene emission respond oppositely to short-term leaf temperature fluctuations. However, both SIF_sp and SIF_st show relatively high monthly correlations with isoprene emissions (r^2=0.55 and 0.50, respectively), indicating that satellite SIF data products may offer an indirect tool to investigate isoprene emission variability at monthly and longer time scales.

Product Name	June			July			August		
	2011	2012	Diff.	2011	2012	Diff.	2011	2012	Diff.
GPP	0.97	0.62	-36% *	0.78	0.20	-74% *	0.65	0.14	-78% *
SIF_sp	1.87	1.89	+0.7%	1.85	1.31	-29% *	1.43	1.15	-19%
SIF_st	2.07	1.76	-14% *	1.91	1.28	-33% *	1.59	1.16	-27% *
Iemis	10.67	11.77	+10%	19.78	9.18	-54% *	10.17	3.37	-67% *
OMI-std	1.29	1.44	+11%	2.01	2.25	+12%	1.68	1.33	-21%
OMI-GC	0.82	0.84	+2%	1.87	1.37	-27%	1.11	0.91	-18%
OMI-IM	1.38	1.27	-8%	1.89	1.66	-12%	1.43	0.95	-33% *
GOME2-IM	1.24	1.10	-11%	1.50	1.41	-6%	1.13	0.79	-30%

Table 2. Monthly average FLUXNET observed GPP (g[C] m^{-2} hr^{-1}), satellite SIF (mW m^{-2} sr^{-1} nm^{-1}), observed isoprene emission (Iemis, mg[C] m^{-2} hr^{-1}) and satellite-based vertical HCHO column concentrations (×10^{16} molecules cm^{-2}) in JJA 2011 and 2012, and their relative difference. The relative difference is calculated as (2012_value – 2011_value) / 2011_value × 100%. The star (*) markers indicate significant 2012-to-2011 differences ($p<0.05$ for student's t-test) with respect to the day-to-day variations within each month.

3.3 Response of atmospheric formaldehyde to severe drought

We use four satellite HCHO column products to understand the HCHO trend (Table 1, Fig. 3). The monthly HCHO column magnitudes among the four products agree relatively well with a spread within a factor of 2 (Table 2). Three products, OMI-GC, OMI-IM and GOME2-IM, successfully capture the HCHO column reductions in July and August 2012 relative to 2011 (Fig. 4), and demonstrate reasonable correlation with the observed monthly mean isoprene emissions (r^2=0.50~0.71). OMI-std indicates higher HCHO column concentrations in July 2012 than 2011, which is inconsistent with the isoprene emission measurements. OMI-std uses the chemistry-transport model GEOS-Chem for processing, but the air mass factors (AMFs) are fixed to year 2007. The product shows weak correlation with observed isoprene emission (r^2=0.18). This result reveals the fundamental importance of AMFs in the application of HCHO satellite-based measurements for atmospheric chemistry research. On daily time scales, only OMI-GC indicates elevated HCHO column concentrations during late July in 2011 when the observed isoprene is

unprecedentedly high (Fig. 2G). However, none of the four products demonstrates a satisfactory or convincing correlation with isoprene emission observations on daily time scales (r^2=0.03~0.22, Fig. 3). At weekly scales, correlations are overall improved using 7-day running means (r^2=0.07~0.40, Fig. 3).

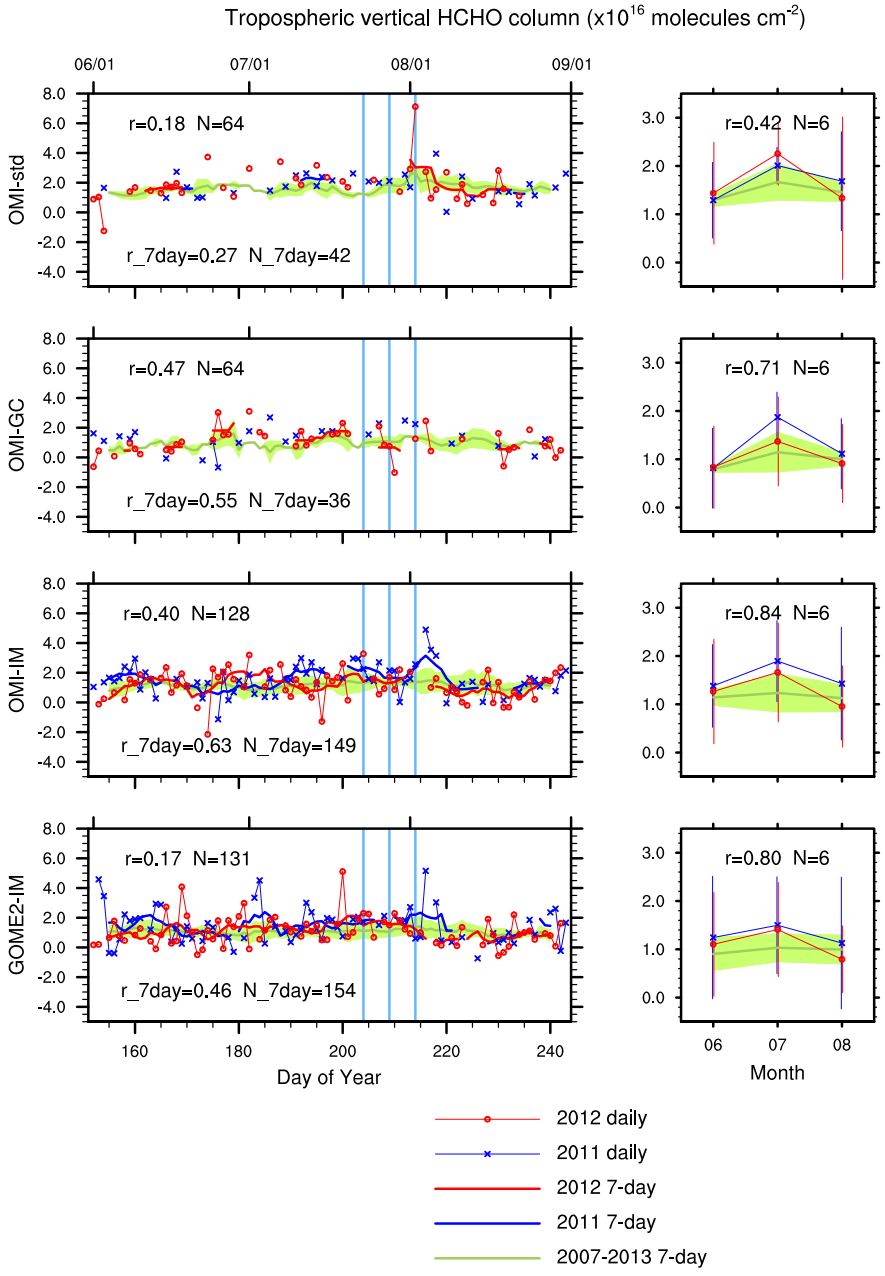

Figure 3. Time-series of daily and monthly tropospheric vertical HCHO column over the MOFLUX site. Green shades represent the multi-year variation of the 7-day running mean values. The correlation coefficients r against site-level isoprene emissions are calculated using daily, 7-day running mean and monthly mean values. The error bars in the monthly plots represent the 1 standard deviation of day-to-day variation within each month.

Although OMI-GC, OMI-IM and GOME2-IM successfully indicate lower HCHO column concentrations in 2012, their 2012-to-2011 differences are not statistically significant with respect to day-to-day variations (p-values > 0.05, Table 2), and are similar to the 1 standard deviation of interannual variability (Fig. 3). These 2012-to-2011 differences of HCHO columns are also relatively less than that of the isoprene emission changes (Table 2). For example, the isoprene emissions in July 2012 are 54% lower than July 2011, while the relative reductions in July for the three HCHO products are 27%, 12% and 6%, respectively. In August 2012, isoprene emission has decreased by 67% compared to August 2011, while the HCHO column reductions are only 18~33%. Moreover, there is a marked disagreement between the isoprene emission and satellite HCHO column intra-seasonal cycles. Isoprene in July 2012 is lower than June 2012 due to the severe drought effect, but all HCHO products show a peak in July every year. Possible reasons related to meteorology for these apparent discrepancies between isoprene emission and satellite HCHO columns include: high temperatures during drought conditions accelerate chemical reaction rates thus facilitating oxidation of isoprene to form HCHO; reduced water vapor concentrations and isoprene emission alter the atmospheric oxidation capacity (i.e. the concentration of OH) and therefore have an effect on the relative changes of isoprene and HCHO. We explore the impacts of these individual drought-altered drivers on oxidation and HCHO in the next section using a photochemical box model.

3.4 Sensitivity of HCHO to drought-altered temperature, water and isoprene emission

We apply the box model BOXMOX [*Knote et al.*, 2014] to examine the impacts of air temperature (T_a), water vapor concentration (H_2O) and isoprene emission (Iemis) on HCHO within boundary layer. In all three summer months (JJA), temperatures are higher and water vapor concentrations are lower in 2012 than in 2011. The control case is driven by observed monthly mean T_a, H_2O and Iemis at their 2011 levels (Case 1, purple bars in Fig. 4). Compared to the control case, changing to high T_a in 2012 leads to a higher OH concentration (Case 2, yellow bars) due to accelerated kinetics. Further changing to smaller H_2O concentration in 2012 brings down the amount of OH (Case 3, green bars) as H_2O is the main source of OH production. The OH changes due to T_a and H_2O differences between 2011 and 2012 can be neglected compared to the effects of isoprene emission changes. In July and August, isoprene in 2012 is substantially lower which leads to a jump in oxidation capacity (Case 4, red bars). This elevated OH oxidizes more volatile organic compounds (VOCs), including monoterpene, methane and anthropogenic VOCs, which also contribute to the formation of HCHO. Such effect is stronger than increases in the HCHO loss by OH oxidation [*Valin et al.*, 2016]. In Case 4, the simulated isoprene concentration in July is reduced by 60% with respect to Case 3, and in August, isoprene is almost completely depleted. In contrast, the relative differences of simulated HCHO column concentrations between Case 4 and Case 3 are -29% and -31% in July and August. The HCHO reductions are smaller than the input isoprene emission reductions. The simplified box model results demonstrate that the elevated oxidation capacity under drought conditions behaves as a "buffer" that leads to the smaller HCHO reductions.

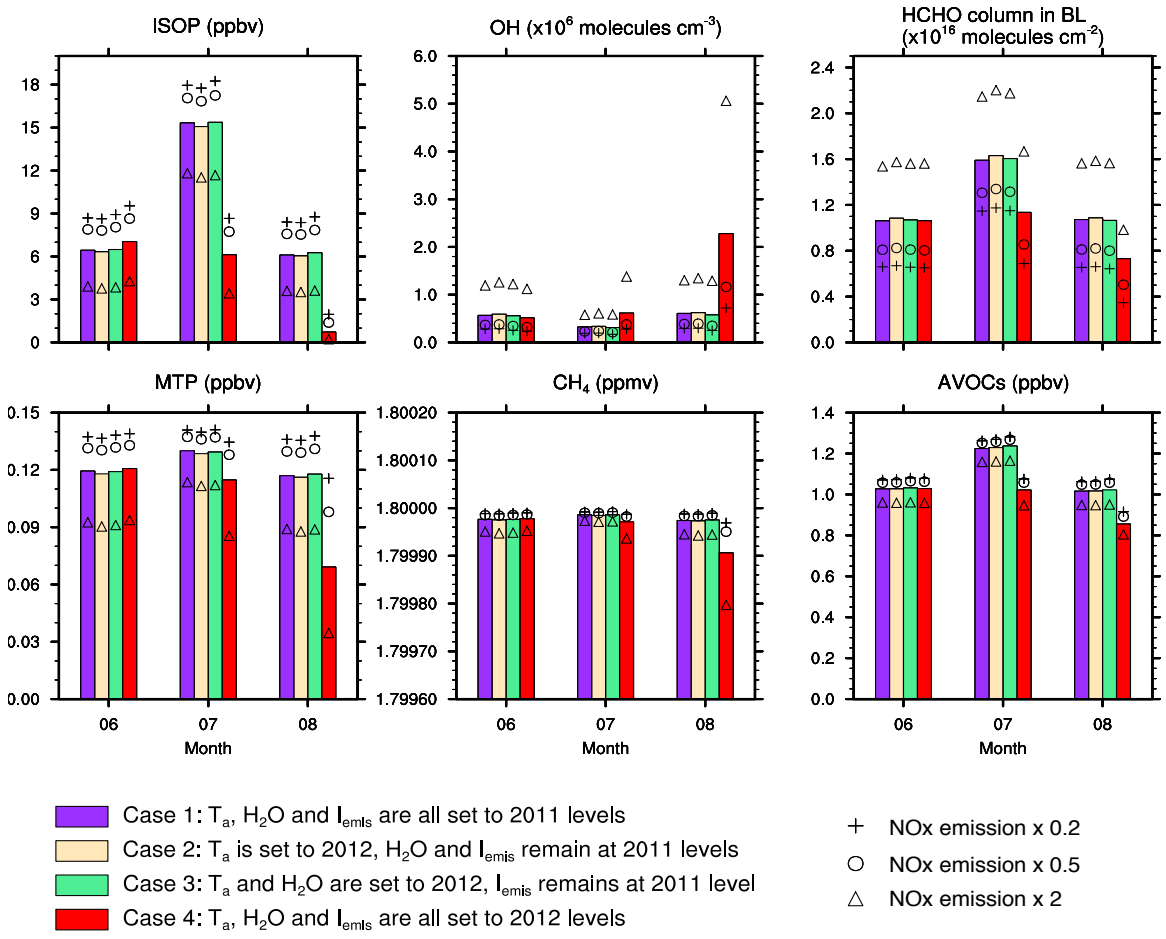

Figure 4. Modeled midday concentrations from the BOXMOX simulations. The box model output concentrations for all species. The HCHO column concentration in the boundary layer (BL) is calculated as the product of HCHO concentration and the prescribed BL height (about 1.5km in midday). The cross, circle and triangle markers represent sensitivity simulations with NEI2005 NO_x emission multiplied by a factor of 0.2, 0.5 and 2, respectively. Abbreviations: ISOP-isoprene concentration, MTP-monoterpene concentration, AVOCs-anthropogenic volatile organic compounds concentration. The units "ppmv" and "ppbv" are equivalent to 2.6×10^{13} molecules cm^{-3} and 2.6×10^{10} molecules cm^{-3}, respectively.

Several factors that may have an impact on HCHO under drought conditions are not tested in these simplified BOXMOX experiments. *Valin et al.* [2016] and *Wolfe et al.* [2016] have shown that for regions like the MOFLUX site with high VOC emissions and low NO_x concentrations, the HCHO columns are more sensitive to OH production rate than isoprene emission. The dependence on NO_x regime may contribute the observed muted HCHO responses but is not able to be tested here due to lack of in-situ NO_x measurements. In the BOXMOX setup, we fix the NO_x emission using the NEI2005 inventory in all months, without differentiating the 2012-to-2011 differences. Additionally we do a series of sensitivity studies by applying a factor of 0.2, 0.5 and 2 to the NO_x emission in all months to consider the uncertainty associate with the NEI2005 NO_x inventory [*Travis et al.*, 2016]. As shown in Fig. 4, our conclusion about the role of oxidation capacity as a chemical "buffer" still holds among all the sensitivity experiments across a variety of NO_x emission ranges.

Other uncertainty sources include the monoterpene emissions and photolysis rates. The response of biogenic monoterpene emissions to drought stress is less well studied than isoprene. Based on a recent study, the monoterpene emission at this site is mostly associated with light-dependent release that generally responds in a manner similar to isoprene emission [*Geron et al.*, 2016]. Therefore monoterpenes could also be reduced during the 2012 long-term drought and further increase the OH level, similar as the isoprene. We do not consider the 2011-2012 monoterpene differences in this box model study. In BOXMOX, monoterpene emissions are fixed to the observed values averaged over JJA 2012 (the only available observations at the MOFLUX site). Photolysis rates are fixed with a typical diurnal cycle for all simulations and do not respond to local measured meteorology. Changing photolysis rates by ±10% results in fluctuations within ±11%, ±6% and ±4% for simulated OH, isoprene and HCHO concentrations, respectively, and do not change our conclusion. In addition, the in-situ measured incoming solar radiation from FLUXNET shows a small increase of 2.5% in summer 2012 compared to 2011, therefore the fixed photolysis rates may have only minor influences on this study. Other physical and chemical factors could be different under drought conditions and affect HCHO columns, too, but are not considered here thus brining uncertainty. These uncertainty sources include changes in vertical mixing, boundary layer height, cloud height and fraction, horizontal advection of HCHO and its precursors, etc.

3.5 Regional-scale implications for satellite SIF and HCHO columns

We show the summertime satellite SIF_st and HCHO columns at regional scale in Fig. 5. We choose the OMI-IM product as an example as it has been shown to have the smallest bias compared to aircraft measurements [*Zhu et al.*, 2016]. The brown contour lines indicate the regions where extremely dry conditions happened in JJA 2011 and 2012, i.e. the standardized precipitation index SPI < -1.6 (as defined in https://www.ncl.ucar.edu/Applications/spi.shtml). The US suffered from an unprecedented drought in 2011 centered in Texas [*Nielson-Gammon*, 2012] and a historical drought in 2012 in the central US [*Rippey*, 2015]. At such seasonal scales (3-month average), the MOFLUX site was not influenced by the 2011 Texas drought but did suffer severe water deficit conditions in 2012, consistent with Fig. 1. SIF_st demonstrates significant reductions during the two seasonal droughts at the same regions (Texas in 2011 and central US in 2012), directly demonstrating the sensitivity of plant photosynthesis to surface water availability, consistent with a previous study [*Sun et al.*, 2015]. Our analysis in Section 3.2 further suggest that such decreases in SIF_st (about -10~-30%) may indicate larger reductions in GPP. In contrast, satellite HCHO columns do not show statistically significant responses to the Texas and central US droughts. In these two regions, isoprene emissions are relatively low and methane and anthropogenic VOCs strongly influence HCHO production. Methane and anthropogenic VOCs are not as sensitive to water availability as biogenic isoprene production. Deriving and analyzing isoprene emissions from satellite HCHO columns needs further model interpretation which is beyond the scope of this study. The high isoprene emission regions, e.g. the southeast US, are not influenced by the two droughts.

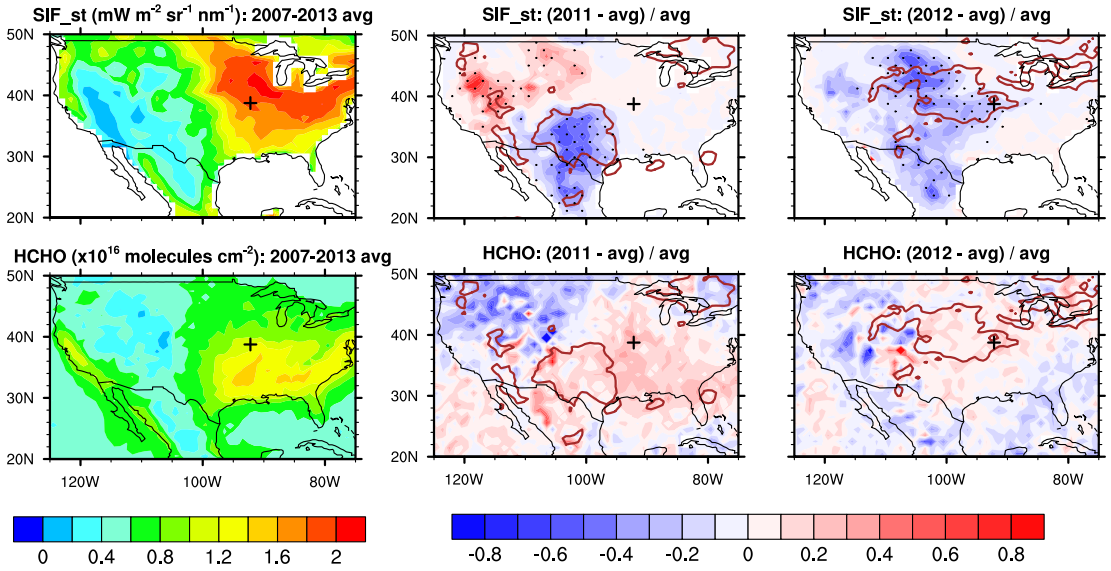

Figure 5. Summertime (JJA mean) satellite SIF_st (mW m^{-2} sr^{-1} nm^{-1}) and OMI-IM tropospheric vertical HCHO columns ($\times 10^{16}$ molecules cm^{-2}) over the US, and the 2011 and 2012 relative differences compared to the 2007-2013 average. Brown contour lines show the regions where the 3-month SPI<-1.6, indicating extreme drought conditions. Dotted shading indicates significant changes with respect to the interannual variations ($p<0.05$).

4. Summary and Discussion

Atmospheric oxidation of isoprene emission has a profound effect on air quality and climate. One of its high-yield intermediate oxidation products, HCHO, can be monitored from space, and as such has been used as a proxy for surface isoprene emission. This vegetation-chemistry linkage is strongly influenced by meteorological conditions and climate, among which drought is one important impact driver. The mid-latitude, oak-dominated forest in Missouri Ozarks in central US suffered a three-month long drought condition in summer 2012 and a mild stress in summer 2011, providing a unique opportunity to study the impacts of different levels of drought on the photosynthesis-isoprene-HCHO system. In this study, we applied site-level derived GPP and remote-sensed SIF as indicators for photosynthetic activity, two in-situ directly measured isoprene emission flux datasets (2011 and 2012), and four satellite-based tropospheric vertical HCHO column datasets to explore the potential of HCHO and SIF as isoprene emission and photosynthesis indicators under drought conditions.

Photosynthesis in the MOFLUX site decreases significantly in summer 2012 especially in July (-29% for SIF_sp, -33% for SIF_st and -97% for GPP compared to 2011). Isoprene emission reduction, about 54% lower than 2011 in July, is a few weeks delayed compared to the photosynthesis reduction. This large reduction in isoprene emission is likely driven by the lack of leaf carbon availability following prolonged reduced photosynthetic activity. In contrast to their similar reductions in summer 2012, the photosynthesis and isoprene emission respond oppositely to a short-term hot and dry period in 2011, especially when related to peak temperatures. Satellite SIF products from GOME2 are able to capture qualitatively the local GPP variations to both mild and severe drought stresses at the MOFLUX site. The SIF_st product processed using spatiotemporal kriging method performs better at reproducing the variability in site-level GPP at

daily, weekly and monthly scales than the SIF_sp product that applies spatial kriging method. The smaller SIF reductions compared to GPP may be because electron transport and photosystem activity is maintained to a certain extent even under severe drought in this ecosystem while metabolic capacity has essentially shut down [*Lawlor and Tezara*, 2009]. The two SIF products also show relatively high correlations with isoprene emissions at monthly scales, potentially providing another indirect approach to examine long-term isoprene emission variations from space.

The reliability of satellite-based HCHO column products to indicate surface isoprene emission highly depends on modeled air mass factors that are used to convert retrieved slant columns to vertical columns. In this study, three of the four HCHO products successfully capture the monthly isoprene reductions in the MOFLUX site under severe drought conditions, all of which use air mass factors from a chemical-transport model with year-to-year variations. On daily to weekly time scales, most HCHO satellite data products are not reliable to detect variations in isoprene emission. Similar to the SIF finding, the monthly HCHO columns show a muted response compared to the isoprene emission reductions, and they all display a peak in July 2012, which is not detected in the isoprene flux observations. The simplified box model results indicate that the muted HCHO response is due to a chemical feedback in altered oxidation capacity whereby reduced isoprene emission increases availability of OH for enhanced HCHO production from other VOC sources, in agreement with a recent assessment [*Valin et al.*, 2016].

At regional scales, SIF_st show significant seasonal reductions in the Texas drought in summer 2011 and the central US drought in summer 2012. Such phenomena directly demonstrate the sensitivity of photosynthesis to surface water availability, and may indicate greater reductions in GPP. Satellite HCHO columns (using OMI-IM as an example) show no significant response to the 2011 Texas drought and the 2012 central US drought at large spatial scales, as the high isoprene emission regions (e.g. the southeast US) are not influenced by the two droughts.

The study is subject to limitations and uncertainties. As previously intimated, structural uncertainties associated with gridded satellite-derived data products, including their model dependence, cloud contamination and spatiotemporal averaging may play a role in their unsatisfactory comparison with in-situ observations. Cloud fraction and types are usually different under drought conditions. Satellite products consider near clear-sky conditions only (e.g. cloud cover < 40%, see details in the literature cited in Table 1 and references therein). Over the MOFLUX site, most HCHO column products have more daily data points passed quality control in the long-drought year 2012 than 2011, indicating fewer cloudy days during drought conditions (associated with less water vapor, stagnant weather conditions, etc). Clouds and aerosols can alter the beam and scatter light reaching the plant leaves thus having a complex impact on photosynthesis and isoprene emissions. The influence of different cloud and aerosol patterns during droughts on the satellite product retrieval are not examined in this study and warrants further analysis. In addition, vertical mixing and planetary boundary layer height (PBLH) are also different under drought conditions. We find a 38% increase in estimated PBLH from MERRA reanalysis in summer 2012 with respect to 2011, which is associated with higher surface temperature and stronger mixing. *Duncan et al.* [2009] showed that the variations of mixed layer height may contribute up to 15% of the HCHO retrieval uncertainty. Such effects are considered in the satellite HCHO retrieval process already but are model-dependent. In general,

the uncertainties associated with OMI products are estimated to be 10-100%, mostly coming from uncertainties in cloud fraction and cloud top pressure, the a priori modeled isoprene emissions, and the HCHO vertical column retrieval (e.g. [*Barkley et al.*, 2013; *González Abad et al.*, 2015]). The GOME2-IM product might be more noisy due to instrument degradation and reduced sampling [*Zhu et al.*, 2016]. Uncertainties also include measurement errors of site-level carbon fluxes and isoprene emission measurements.

In conclusion, our results suggest that satellite SIF and HCHO data products qualitatively capture drought effects on plant carbon fluxes at weekly to monthly scales, but with smaller responses. Caution is needed when using satellite products to detect drought impacts on land carbon fluxes. For instance, quite moderate reductions in satellite SIF and HCHO column may imply much larger reductions in photosynthesis and isoprene emission in reality, which has not been explicitly emphasized by previous literature. Long-term observations of plant carbon fluxes and VOC emissions co-located with soil moisture monitoring in different biomes are needed to improve further process-based understanding of the coupling and decoupling between photosynthesis and isoprene emission.

Acknowledgements

We acknowledge computational support from the Yale University Faculty of Arts and Sciences High Performance Computing Center. Y. Z. thanks National Aeronautics and Space Administration (NASA) for a graduate Earth and Space Sciences Fellowship and a Doctoral Dissertation Improvement Grant from Yale Institute for Biospheric Studies. R. S. thanks Fundación Ramón Areces for a postdoctoral fellowship. M. P. B. acknowledges the usage of the ALICE and SPECTRE High Performance Computing Facility at the University of Leicester. The development of the gridded SIF dataset was supported by NASA through grants No. NNX12AB90G and NNX13AC48G, and the National Science Foundation (NSF) through grant No. 1342076. We acknowledge the free use of tropospheric HCHO column data from OMI and GOME-2 sensors from http://h2co.aeronomie.be/. All data for this paper are properly cited and accredited in the reference list.

Reference:

Affek, H. P., and D. Yakir (2003), Natural abundance carbon isotope composition of isoprene reflects incomplete coupling between isoprene synthesis and photosynthetic carbon flow., *Plant Physiol.*, *131*, 1727–1736, doi:10.1104/pp.102.012294.

Báez, A. P., H. G. Padilla, and R. D. Belmont (1993), Scavenging of atmospheric formaldehyde by wet precipitation, *Environ. Pollut.*, *79*(3), 271–275, doi:10.1016/0269-7491(93)90100-3.

Baldocchi, D. et al. (2001), FLUXNET: A New Tool to Study the Temporal and Spatial Variability of Ecosystem-Scale Carbon Dioxide, Water Vapor, and Energy Flux Densities, *Bull. Am. Meteorol. Soc.*, *82*(11), 2415–2434, doi:10.1175/1520-0477(2001)082<2415:FANTTS>2.3.CO;2.

Barkley, M. P., P. I. Palmer, U. Kuhn, J. Kesselmeier, K. Chance, T. P. Kurosu, R. V. Martin, D. Helmig, and A. Guenther (2008), Net ecosystem fluxes of isoprene over tropical South America inferred from Global Ozone Monitoring Experiment (GOME) observations of HCHO columns, *J. Geophys. Res. Atmos.*, *113*, 1–24, doi:10.1029/2008JD009863.

Barkley, M. P. et al. (2013), Top-down isoprene emissions over tropical South America inferred from SCIAMACHY and OMI formaldehyde columns, *J. Geophys. Res. Atmos.*, *118*(12), 6849–6868, doi:10.1002/jgrd.50552.

Bey, I., D. J. Jacob, R. M. Yantosca, J. A. Logan, B. D. Field, A. M. Fiore, Q.-B. Li, H.-Y. Liu, L. J. Mickley, and M. G. Schultz (2001), Global Modeling of Tropospheric Chemistry with Assimilated Meteorology: Model Description and Evaluation, *J. Geophys. Res.*, *106*, 73–95, doi:10.1029/2001JD000807.

Brüggemann, N., and J. P. Schnitzler (2002), Comparison of isoprene emission, intercellular isoprene concentration and photosynthetic performance in water-limited oak (Quercus pubescens Willd. and Quercus robur L.) saplings, *Plant Biol.*, *4*(4), 456–463, doi:10.1055/s-2002-34128.

Carlton, A. G., and K. R. Baker (2011), Photochemical modeling of the Ozark isoprene volcano: MEGAN, BEIS, and their impacts on air quality predictions., *Environ. Sci. Technol.*, *45*(10), 4438–4445, doi:10.1021/es200050x.

Carslaw, K. S., O. Boucher, D. V Spracklen, G. W. Mann, J. G. L. Rae, S. Woodward, and M. Kulmala (2010), A review of natural aerosol interactions and feedbacks within the Earth system, *Atmos. Chem. Phys.*, *10*(4), 1701–1737.

Cook, B. I., J. E. Smerdon, R. Seager, and S. Coats (2014), Global warming and 21st century drying, *Clim. Dyn.*, *43*(9–10), 2607–2627, doi:10.1007/s00382-014-2075-y.

Delwiche, C. F., and T. D. Sharkey (1993), Rapid appearance of 13C in biogenic isoprene when 13CO2 is fed to intact leaves, *Plant. Cell Environ.*, *650*(16), 587–591, doi:Doi 10.1111/J.1365-3040.1993.Tb00907.X.

Duncan, B. N., Y. Yoshida, M. R. Damon, A. R. Douglass, and J. C. Witte (2009), Temperature dependence of factors controlling isoprene emissions, *Geophys. Res. Lett.*, *36*(5), 1–5, doi:10.1029/2008GL037090.

622 Emmons, L. K., S. Walters, P. G. Hess, J. Lamarque, G. G. Pfister, D. Fillmore, and C. Granier
623 (2010), Model Development Description and evaluation of the Model for Ozone and
624 Related chemical Tracers , version 4 (MOZART-4), , 43–67.

625 Fall, R., and R. K. Monson (1992), Isoprene emission rate and intercellular isoprene
626 concentration as influenced by stomatal distribution and conductance., *Plant Physiol.*,
627 *100*(2), 987–992, doi:10.1104/pp.100.2.987.

628 Frankenberg, C. et al. (2011), New global observations of the terrestrial carbon cycle from
629 GOSAT: Patterns of plant fluorescence with gross primary productivity, *Geophys. Res.*
630 *Lett.*, *38*(17), n/a-n/a, doi:10.1029/2011GL048738.

631 Fu, T.-M., D. J. Jacob, P. I. Palmer, K. Chance, Y. X. Wang, B. Barletta, D. R. Blake, J. C.
632 Stanton, and M. J. Pilling (2007), Space-based formaldehyde measurements as constraints
633 on volatile organic compound emissions in east and south Asia and implications for ozone,
634 *J. Geophys. Res.*, *112*(D6), D06312, doi:10.1029/2006JD007853.

635 Funk, J. L., C. G. Jones, D. W. Gray, H. L. Throop, L. a. Hyatt, and M. T. Lerdau (2005),
636 Variation in isoprene emission from Quercus rubra: Sources, causes, and consequences for
637 estimating fluxes, *J. Geophys. Res. D Atmos.*, *110*(4), 1–10, doi:10.1029/2004JD005229.

638 Garbulsky, M. F., I. Filella, A. Verger, and J. Peñuelas (2014), Photosynthetic light use
639 efficiency from satellite sensors: From global to Mediterranean vegetation, *Environ. Exp.*
640 *Bot.*, *103*, 3–11, doi:10.1016/j.envexpbot.2013.10.009.

641 Geron, C., R. Daly, P. Harley, R. Rasmussen, R. Seco, A. Guenther, T. Karl, and L. Gu (2016),
642 Large drought-induced variations in oak leaf volatile organic compound emissions during
643 PINOT NOIR 2012, *Chemosphere*, *146*, 8–21, doi:10.1016/j.chemosphere.2015.11.086.

644 González Abad, G., X. Liu, K. Chance, H. Wang, T. P. Kurosu, and R. Suleiman (2015),
645 Updated Smithsonian Astrophysical Observatory Ozone Monitoring Instrument (SAO OMI)
646 formaldehyde retrieval, *Atmos. Meas. Tech.*, *8*, 19–32, doi:10.5194/amt-8-19-2015.

647 Gu, L., T. Meyers, S. G. Pallardy, P. J. Hanson, B. Yang, M. Heuer, K. P. Hosman, J. S. Riggs,
648 D. Sluss, and S. D. Wullschleger (2006), Direct and indirect effects of atmospheric
649 conditions and soil moisture on surface energy partitioning revealed by a prolonged drought
650 at a temperate forest site, *J. Geophys. Res.*, *111*(D16102), doi:10.1029/2006JD007161.

651 Gu, L., S. G. Pallardy, K. P. Hosman, and Y. Sun (2015), Drought-influenced mortality of tree
652 species with different predawn leaf water dynamics in a decade-long study of a central US
653 forest, *Biogeosciences*, *12*, 2831–2845, doi:10.5194/bg-12-2831-2015.

654 Gu, L., S. G. Pallardy, K. P. Hosman, and Y. Sun (2016), Agricultural and Forest Meteorology
655 Impacts of precipitation variability on plant species and community water stress in a
656 temperate deciduous forest in the central US □, *Agric. For. Meteorol.*, *217*, 120–136,
657 doi:10.1016/j.agrformet.2015.11.014.

658 Guanter, L. et al. (2014), Global and time-resolved monitoring of crop photosynthesis with
659 chlorophyll fluorescence., *Proc. Natl. Acad. Sci. U. S. A.*, *111*(14), E1327-33,
660 doi:10.1073/pnas.1320008111.

661 Guenther, A. B., T. Karl, P. Harley, C. Wiedinmyer, P. I. Palmer, and C. Geron (2006),

662 Estimates of global terrestrial isoprene emissions using MEGAN (Model of Emissions of
663 Gases and Aerosols from Nature), *Atmos. Chem. Phys.*, *6*, 3181–3210, doi:doi:10.5194/acp-
664 6-3181-2006.

665 Guttman, N. B. (1999), Accepting the Standardized Precipitation Index: a Calculation
666 Algorithm1, *JAWRA J. Am. Water Resour. Assoc.*, *35*(2), 311–322, doi:10.1111/j.1752-
667 1688.1999.tb03592.x.

668 Heald, C. L., and D. V. Spracklen (2015), Land use change impacts on air quality and climate,
669 *Chem. Rev.*, *115*(10), 4476–4496.

670 Joiner, J., L. Guanter, R. Lindstrot, M. Voigt, a P. Vasilkov, E. M. Middleton, K. F. Huemmrich,
671 Y. Yoshida, and C. Frankenberg (2013), Global monitoring of terrestrial chlorophyll
672 fluorescence from moderate spectral resolution near-infrared satellite measurements:
673 methodology, simulations, and application to GOME-2, *Atmos. Meas. Tech.*, *6*, 2803–2823,
674 doi:10.5194/amt-6-2803-2013.

675 Karl, T., R. Fall, T. N. Rosenstiel, P. Prazeller, B. Larsen, G. Seufert, and W. Lindinger (2002),
676 On-line analysis of the (CO2)-C-13 labeling of leaf isoprene suggests multiple subcellular
677 origins of isoprene precursors, *Planta*, *215*(6), 894–905, doi:Doi 10.1007/S00425-002-
678 0825-2.

679 Knote, C. et al. (2014), Influence of the choice of gas-phase mechanism on predictions of key
680 gaseous pollutants during the AQMEII phase-2 intercomparison, *Atmos. Environ.*, *115*,
681 553–568, doi:10.1016/j.atmosenv.2014.11.066.

682 Lamarque, J. F. et al. (2012), CAM-chem: Description and evaluation of interactive atmospheric
683 chemistry in the Community Earth System Model, *Geosci. Model Dev.*, *5*(3), 369–411,
684 doi:10.5194/gmd-5-369-2012.

685 Lawlor, D. W., and W. Tezara (2009), Causes of decreased photosynthetic rate and metabolic
686 capacity in water-deficient leaf cells: A critical evaluation of mechanisms and integration of
687 processes, *Ann. Bot.*, *103*(4), 561–579, doi:10.1093/aob/mcn244.

688 Lee, J.-E., J. a. Berry, C. van der Tol, X. Yang, L. Guanter, A. Damm, I. Baker, and C.
689 Frankenberg (2015), Simulations of chlorophyll fluorescence incorporated into the
690 Community Land Model version 4, *Glob. Chang. Biol.*, *21*(9), 3469–3477,
691 doi:10.1111/gcb.12948.

692 Marais, E. a. et al. (2012), Isoprene emissions in Africa inferred from OMI observations of
693 formaldehyde columns, *Atmos. Chem. Phys.*, *12*(1995), 6219–6235, doi:10.5194/acp-12-
694 6219-2012.

695 Meroni, M., M. Rossini, L. Guanter, L. Alonso, U. Rascher, R. Colombo, and J. Moreno (2009),
696 Remote sensing of solar-induced chlorophyll fluorescence: Review of methods and
697 applications, *Remote Sens. Environ.*, *113*(10), 2037–2051, doi:10.1016/j.rse.2009.05.003.

698 Monson, R. K. et al. (2007), Isoprene emission from terrestrial ecosystems in response to global
699 change: minding the gap between models and observations., *Philos. Trans. A. Math. Phys.
700 Eng. Sci.*, *365*(1856), 1677–1695, doi:10.1098/rsta.2007.2038.

701 Muller, J.-F., and T. Stavrakou (2005), Inversion of CO and NOx emissions using the adjoint of

the IMAGES model, *Atmos. Chem. Phys.*, *5*, 1157–1186, doi:10.5194/acp-5-1157-2005.

Nielson-Gammon, J. W. (2012), The 2011 Texas drought, *Texas Water J.*, *3*(1), 59–95, doi:10.1061/9780784412312.246.

Niinemets, Ü. (2010), Mild versus severe stress and BVOCs: thresholds, priming and consequences, *Trends Plant Sci.*, *15*(December), 145–153, doi:10.1016/j.tplants.2009.11.008.

Palmer, P. I. et al. (2006), Quantifying the seasonal and interannual variability of North American isoprene emissions using satellite observations of the formaldehyde column, *J. Geophys. Res.*, *111*(D12), doi:10.1029/2005JD006689.

Parazoo, N. C., K. Bowman, J. B. Fisher, C. Frankenberg, D. B. A. Jones, A. Cescatti, Ó. Pérez-Priego, G. Wohlfahrt, and L. Montagnani (2014), Terrestrial gross primary production inferred from satellite fluorescence and vegetation models, *Glob. Chang. Biol.*, doi:10.1111/gcb.12652.

Pegoraro, E., A. Rey, G. Barron-Gafford, R. Monson, Y. Malhi, and R. Murthy (2005), The interacting effects of elevated atmospheric CO2 concentration, drought and leaf-to-air vapour pressure deficit on ecosystem isoprene fluxes, *Oecologia*, *146*(1), 120–129, doi:10.1007/s00442-005-0166-5.

Potosnak, M. J., L. LeStourgeon, S. G. Pallardy, K. P. Hosman, L. Gu, T. Karl, C. Geron, and A. B. Guenther (2014), Observed and modeled ecosystem isoprene fluxes from an oak-dominated temperate forest and the influence of drought stress, *Atmos. Environ.*, *84*, 314–322, doi:10.1016/j.atmosenv.2013.11.055.

Reichstein, M. et al. (2005), On the separation of net ecosystem exchange into assimilation and ecosystem respiration: Review and improved algorithm, *Glob. Chang. Biol.*, *11*(9), 1424–1439, doi:10.1111/j.1365-2486.2005.001002.x.

Rienecker, M. M. et al. (2011), MERRA: NASA's Modern-Era Retrospective Analysis for Research and Applications, *J. Clim.*, *24*(14), 3624–3648, doi:Doi 10.1175/Jcli-D-11-00015.1.

Rippey, B. R. (2015), The U.S. drought of 2012, *Weather Clim. Extrem.*, *10*, 57–64, doi:10.1016/j.wace.2015.10.004.

Ryan, A. C., C. N. Hewitt, M. Possell, C. E. Vickers, A. Purnell, P. M. Mullineaux, W. J. Davies, and I. C. Dodd (2014), Isoprene emission protects photosynthesis but reduces plant productivity during drought in transgenic tobacco (Nicotiana tabacum) plants, *New Phytol.*, *201*(1), 205–216, doi:10.1111/nph.12477.

Seco, R., T. Karl, A. Guenther, K. P. Hosman, S. G. Pallardy, L. Gu, C. Geron, P. Harley, and S. Kim (2015), Ecosystem-scale volatile organic compound fluxes during an extreme drought in a broadleaf temperate forest of the Missouri Ozarks (central USA), *Glob. Chang. Biol.*, *21*, 3657–3674, doi:10.1111/gcb.12980.

Sharkey, T. D., and F. Loreto (1993), Water stress, temperature, and light effects on the capacity for isoprene emission and photosynthesis of kudzu leaves, *Oecologia*, *95*(3), 328–333, doi:10.1007/BF00320984.

De Smedt, I., M. Van Roozendael, T. Stavrakou, J. F. M??ller, C. Lerot, N. Theys, P. Valks, N. Hao, and R. Van Der A (2012), Improved retrieval of global tropospheric formaldehyde columns from GOME-2/MetOp-A addressing noise reduction and instrumental degradation issues, *Atmos. Meas. Tech.*, *5*(11), 2933–2949, doi:10.5194/amt-5-2933-2012.

De Smedt, I. et al. (2015), Diurnal, seasonal and long-term variations of global formaldehyde columns inferred from combined OMI and GOME-2 observations, *Atmos. Chem. Phys.*, *15*(21), 12519–12545, doi:10.5194/acp-15-12519-2015.

Sun, Y., R. Fu, R. Dickinson, J. Joiner, C. Frankenberg, L. Gu, Y. Xia, and N. Fernando (2015), Drought onset mechanisms revealed by satellite solar-induced chlorophyll fluorescence: Insights from two contrasting extreme events, *J. Geophys. Res. G Biogeosciences*, *120*(11), 2427–2440, doi:10.1002/2015JG003150.

Tadić, J. M., X. Qiu, V. Yadav, and A. M. Michalak (2015), Mapping of satellite Earth observations using moving window block kriging, *Geosci. Model Dev.*, *8*, 3311–3319, doi:10.5194/gmd-8-3311-2015.

Tadić, J. M., X. Qiu, S. Miller, and A. M. Michalak (2017), Spatio-temporal approach to moving window block kriging of satellite data, *Geosci. Model Dev.*, *10*, 709–720, doi:10.5194/gmd-2016-192.

Tilmes, S. et al. (2015), Description and evaluation of tropospheric chemistry and aerosols in the Community Earth System Model (CESM1.2), *Geosci. Model Dev.*, *8*(5), 1395–1426, doi:10.5194/gmd-8-1395-2015.

Travis, K. R. et al. (2016), Why do models overestimate surface ozone in the Southeast United States ?, *Atmos. Chem. Phys.*, *16*, 13561–13577, doi:10.5194/acp-16-13561-2016.

Unger, N. (2014a), Human land-use-driven reduction of forest volatiles cools global climate, *Nat. Clim. Chang.*, doi:10.1038/nclimate2347.

Unger, N. (2014b), On the role of plant volatiles in anthropogenic global climate change, *Geophys. Res. Lett.*, *41*, 8563–8569, doi:doi:10.1002/2014GL061616.

Valin, L. C., A. M. Fiore, K. Chance, and G. G. Abad (2016), The role of OH production in interpreting the variability of Ch2O columns in the southeast U.S., *J. Geophys. Res.*, *121*, 478–493, doi:10.1002/2015JD024012.Received.

Voigt, M., L. Guanter, Y. Zhang, S. Walther, P. Kohler, and M. Jung (2009), Global Analysis of the Relationship between Canopy-Scale Chlorophyll Fluorescence and GPP, *Biogeosciences*, *6*(12), 3109–3129.

Walther, S., M. Voigt, T. Thum, A. Gonsamo, Y. Zhang, P. K??hler, M. Jung, A. Varlagin, and L. Guanter (2016), Satellite chlorophyll fluorescence measurements reveal large-scale decoupling of photosynthesis and greenness dynamics in boreal evergreen forests, *Glob. Chang. Biol.*, *22*(9), 2979–2996, doi:10.1111/gcb.13200.

Wiedinmyer, C. et al. (2005), Ozarks Isoprene Experiment (OZIE): Measurements and modeling of the "isoprene volcano," *J. Geophys. Res. D Atmos.*, *110*(18), D18307, doi:10.1029/2005JD005800.

Wolfe, G. M., J. Kaiser, T. F. Hanisco, F. N. Keutsch, J. A. De Gouw, J. B. Gilman, M. Graus,

782 and C. D. Hatch (2016), Formaldehyde production from isoprene oxidation across NO x
783 regimes, *Atmos. Chem. Phys.*, *16*(x), 2597–2610, doi:10.5194/acp-16-2597-2016.

784 Xu, L., S. S. Saatchi, Y. Yang, R. B. Myneni, C. Frankenberg, D. Chowdhury, and J. Bi (2015),
785 Satellite observation of tropical forest seasonality: spatial patterns of carbon exchange in
786 Amazonia, *Environ. Res. Lett.*, *10*(8), 84005, doi:10.1088/1748-9326/10/8/084005.

787 Yang, X., J. Tang, J. F. Mustard, J. Lee, and M. Rossini (2015), Geophysical Research Letter
788 Supplementary information for " Solar-induced chlorophyll fluorescence correlates with
789 canopy photosynthesis on diurnal and seasonal scales in a temperate deciduous forest ,"
790 *Geophys. Res. Lett.*, *42*, 2977–2987, doi:10.1002/2015GL063201.

791 Yoshida, Y., J. Joiner, C. Tucker, J. Berry, J. E. Lee, G. Walker, R. Reichle, R. Koster, A.
792 Lyapustin, and Y. Wang (2015), The 2010 Russian drought impact on satellite
793 measurements of solar-induced chlorophyll fluorescence: Insights from modeling and
794 comparisons with parameters derived from satellite reflectances, *Remote Sens. Environ.*,
795 *166*, 163–177, doi:10.1016/j.rse.2015.06.008.

796 Zheng, Y., N. Unger, A. Hodzic, L. Emmons, C. Knote, S. Tilmes, J. F. Lamarque, and P. Yu
797 (2015a), Limited effect of anthropogenic nitrogen oxides on secondary organic aerosol
798 formation, *Atmos. Chem. Phys.*, *15*(23), 13487–13506, doi:10.5194/acp-15-13487-2015.

799 Zheng, Y., N. Unger, M. P. Barkley, and X. Yue (2015b), Relationships between photosynthesis
800 and formaldehyde as a probe of isoprene emission, *Atmos. Chem. Phys.*, *15*, 8559–8576,
801 doi:10.5194/acp-15-8559-2015.

802 Zhu, L. et al. (2016), Observing atmospheric formaldehyde (HCHO) from space : validation
803 and intercomparison of six retrievals from four satellites (OMI , GOME2A , GOME2B ,
804 OMPS) with SEAC 4 RS aircraft observations over the Southeast US, *Atmos. Chem. Phys.*
805 *Discuss.*, (March), 1–24, doi:10.5194/acp-2016-162.

806